The American Journal of Pathology, Vol. 181, No. 2, August 2012

http://dx.doi.org/10.1016/j.ajpath.2012.05.009

Immunopathology and Infectious Diseases

Activated B Cells in the Granulomas of Nonhuman Primates Infected with *Mycobacterium tuberculosis*

Jia Yao Phuah,* Joshua T. Mattila,* Philana L. Lin,† and JoAnne L. Flynn*

From the Department of Microbiology and Molecular Genetics, University of Pittsburgh School of Medicine, Pittsburgh; and the Department of Pediatrics,† Children's Hospital of Pittsburgh, University of Pittsburgh Medical Center, Pittsburgh, Pennsylvania*

In an attempt to contain *Mycobacterium tuberculosis*, host immune cells form a granuloma as a physical and immunological barrier. To date, the contribution of humoral immunity, including antibodies and specific functions of B cells, to *M. tuberculosis* infection in humans remains largely unknown. Recent studies in mice show that humoral immunity can alter *M. tuberculosis* infection outcomes. *M. tuberculosis* infection in cynomolgus macaques recapitulates essentially all aspects of human tuberculosis. As a first step toward understanding the importance of humoral immunity to control of *M. tuberculosis* infection in primates, we characterized the B-cell and plasma-cell populations in infected animals and found that B cells are present primarily in clusters within the granuloma. The B-cell clusters are in close proximity to peripheral node addressin-positive cells and contain cells positive for Ki-67, a proliferation marker. Granuloma B cells also express CXCR5 and have elevated HLA-DR expression. Tissues containing *M. tuberculosis* bacilli had higher levels of *M. tuberculosis*-specific IgG, compared with uninvolved tissue from the same monkeys. Plasma cells detected within the granuloma produced mycobacteria-specific antibodies. Together, these data demonstrate that B cells are present and actively secreting antibodies specific for *M. tuberculosis* antigens at the site of infection, including lung granulomas and thoracic lymph nodes. These antibodies likely have the capacity to modulate local control of infection in tissues. *(Am J Pathol 2012, 181: 508–514; http://dx.doi.org/10.1016/j.ajpath.2012.05.009)*

Mycobacterium tuberculosis is an intracellular pathogen that is the causative agent of tuberculosis (TB), an infection that is estimated to affect a third of the world's population. Ten percent of infected individuals develop clinical symptoms of active TB; the remainder develop latent infection, which is clinically asymptomatic but can reactivate to cause active TB.[1–3] In response to *M. tuberculosis* infection, the host immune system forms an organized conglomeration of cells known as a granuloma. Granulomas are crucial in control of mycobacterial pathogens, because they function as an immune and physical barrier to prevent widespread bacterial dissemination within the host.[4] Proper control of *M. tuberculosis* requires immune cells within the granuloma to kill internalized bacilli by activating macrophages while simultaneously balancing anti-inflammatory signals to reduce tissue damage. T cells in particular play a critical role in activating macrophages via the release of interferon gamma (IFN-γ) and tumor necrosis factor (TNF).[5,6] The contribution of B cells to control of human *M. tuberculosis* infection and pathology remains unknown.

Upon activation by antigen, mature B cells proliferate and differentiate into plasma cells for the sole purpose of generating antigen-specific antibodies. Antibodies can affect host-pathogen interactions by enhancing phagocytosis and antibody-dependent cell cytotoxicity, as well as by blocking pathogen-host receptor interactions.[7,8] Antibody-mediated phagocytosis can modify macrophage behavior, depending on how the Fc portion of antibodies interacts with the Fc receptors expressed on macrophages.[9,10] B cells also present antigen to T cells and enhance $CD4^+$ antigen-specific T-cell expansion.[11,12] B-cell depletion slows disease progression of what are predominantly T-cell-mediated autoimmune conditions, including multiple sclerosis[13,14] and type 1 diabetes,[15] in mice and in humans. These studies reinforce the notion that B-cell antigen presentation is capable of mediating further effects on T cells to drive immune activation in the presence of antigen.

Because *M. tuberculosis* is primarily an intracellular bacillus, the contribution of humoral immunity to protec-

Supported by the Bill and Melinda Gates Foundation and by the NIH (R01-HL68526, R01-HL075845, and R01-AI094745 to J.L.F.).

Accepted for publication May 2, 2012.

Address reprint requests to JoAnne L. Flynn, Ph.D., Microbiology and Molecular Genetics, W1144 BST, 200 Lothrop St., University of Pittsburgh, Pittsburgh, PA 15261. E-mail: joanne@pitt.edu.

tion was thought to be minimal. Studies in the late 19th and early 20th centuries on the protective effects of passive immunization yielded conflicting results, which have been attributed to variations in antisera preparation.[16] *M. tuberculosis* infection of B-cell-deficient mice have also yielded varied findings, ranging from increased pathology or bacterial burden to no apparent change in disease progression.[17,18] The inconsistencies in these mouse studies make it difficult to ascertain the role of the humoral response against TB in humans. Several studies, however, have indicated that other components of the humoral response, including Fc receptors,[19] polymeric Ig receptors,[20] and intravenous immunoglobulin,[21] can affect the outcome of *M. tuberculosis* infection in mice. These studies suggest that B-cell responses can confer protection against *M. tuberculosis* infection either directly or by modulating cellular immune responses (eg, macrophages and T-cell priming and activation).

In the mouse model of *M. tuberculosis* infection, B cells are present in the lungs, often in aggregates that stain positive for peanut agglutinin (PNA), reminiscent of germinal centers in lymph nodes.[17,22] Some studies have suggested that granulomas may also function as tertiary germinal centers, where the T-cell population is continuously activated via antigen presentation by B cells. Although B-cell aggregates have been identified in human lung tissue from TB patients,[23,24] how these B-cell aggregates function in the context of *M. tuberculosis* control is still unknown.

Our objective in the present study was to determine the characteristics of B cells and plasma cells within granulomas of *M. tuberculosis*-infected cynomolgus macaques. This nonhuman primate (NHP) model of *M. tuberculosis* infection has been shown to mimic all aspects of human TB, particularly in granuloma type and structure.

Materials and Methods

Experimental Animals

The study sample was 14 adult (>4 years of age) cynomolgus macaques (*Macaca fascicularis*) obtained from Covance (Alice, TX) and from Valley Biosystems (West Sacramento, CA) and experimentally infected with *M. tuberculosis* for other studies. All animals were housed under biosafety level 3 conditions. These studies followed all applicable animal experimentation guidelines, and all experimental manipulations and protocols were approved by the University of Pittsburgh School of Medicine Institutional Animal Care and Use Committee.

M. tuberculosis *Infection*

Cynomolgus macaques were infected with 25 to 200 CFU of the Erdman strain of *M. tuberculosis* via intrabronchial instillation, as described previously.[25,26] Infection was confirmed by conversion of negative to positive tuberculin skin test and by elevated peripheral blood mononuclear cell responses to mycobacterial antigens relative to baseline, as determined via lymphocyte proliferation assay (LPA) and enzyme-linked immunosorbent spot (ELISPOT) assay.[26,27] Tissue samples for the present study were obtained from *M. tuberculosis*-infected control monkeys used in other TB studies.

Necropsy Procedures

Monkeys were euthanized using pentobarbital and phenytoin (Beuthanasia; Schering-Plough Animal Health, Kenilworth, NJ) and were maximally bled before necropsy. Gross pathological findings were described by a board-certified veterinary pathologist (E.K.) and were classified as described previously.[25,26] Representative sections of each tissue were placed in formalin for histological analysis or were homogenized into single-cell suspensions for immunological studies, flow cytometric analysis, and bacterial burden, as described previously.[25–27] Bone marrow was obtained from the sternum by flushing exposed bone marrow with tissue-grade 1× PBS (Lonza, Walkersville, MD) using a 20-gauge needle (BD, Franklin Lakes, NJ). Red blood cells were lysed using BD Pharm Lyse buffer (BD Biosciences, San Diego, CA), according to the manufacturer's instructions, before cell enumeration. Tissue homogenates from numerous necropsy samples were serially diluted and plated on 7H11 agar medium (BD, Sparks, MD); CFUs were enumerated on day 21. Lung samples with culturable *M. tuberculosis* were classed as involved tissue and samples with no such culturable bacteria were classed as noninvolved. Lymph-node tissues were classified based on anatomical location, with thoracic lymph nodes classed as lung-draining (dLN) and other lymph nodes as peripheral (pLN).

Histological Analysis and Immunohistochemistry

Tissue sections were embedded with paraffin and stained with H&E. These sections were then reviewed microscopically by a veterinary pathologist (E.K.), with specific emphasis on granuloma characteristics, as described previously.[27] Serial sections were used for immunohistochemistry staining of cell markers. Briefly, slides were processed in antigen retrieval buffer (Tris base, 0.05% Tween 20, pH 9) before staining. Antibodies used for staining were anti-human CD20 (rabbit polyclonal; Neomarkers, Fremont, CA), anti-human CD3 (rabbit polyclonal; Dako, Carpinteria, CA), anti-human Ki-67 (rabbit polyclonal; Neomarkers), anti-mouse peripheral node addressin (PNAd) (clone MECA-79; BioLegend, San Diego, CA), anti-rhesus CXCR5 (mouse monoclonal; NIH Nonhuman Primate Reagent Resource, Boston, MA), anti-human CD138 (clone MI5; Neomarkers), and biotinylated PNA (Vector Laboratories, Burlingame, CA). Cell nuclei were stained with DRAQ5 (Biostatus, Shepshed, UK). Slides were preserved using ProLong Gold antifade reagent with DAPI (Invitrogen-Life Technologies, Carlsbad, CA) before visualization under an upright confocal laser scanning microscope (Olympus FluoView 500, model BXL21).

For plasma cell detection, fresh tissues were fixed in freshly prepared 4% paraformaldehyde for 6 hours at 37°C, washed with 1× PBS, and dehydrated in sucrose solution (30% sucrose, 1× PBS) overnight at 4°C. The

tissue was then frozen with cold isobutanol in liquid nitrogen. The frozen tissue was embedded in Tissue-Tek optimal cutting temperature compound (Sakura Finetek, Torrance, CA), and 8-μm sections were cut using a cryostat microtome (model HM505N; Microm International, Walldorf, Germany) at −20°C. Sections were placed on gelatin-coated slides and air-dried overnight at 37°C. The slides were then stained directly, as described above.

Flow Cytometry Analysis of Surface Markers and Quantification of B Cells within Tissue

Single-cell suspensions were derived from granulomatous lung, normal lung, dLN, and pLN. Cells from these tissue samples were stained for T cells using anti-human CD3 (clone SP34-2; BD Biosciences) and for B cells using anti-human CD20 (clone 2H7; eBioscience, San Diego, CA) and T-cell costimulatory molecules CD86 (clone 2331; BD Pharmingen) and HLA-DR (clone LN3; eBioscience). Lymphocytes were identified based on size (forward scatter) and granularity (side scatter). B cells and T cells were further identified based on $CD20^+$ and $CD3^+$ expression, respectively. Further characterization for HLA-DR and CD86 were performed within the $CD20^+$ population. B-cell numbers within tissue were calculated by multiplying the percentage of $CD20^+$ as obtained from flow cytometry, with total cell numbers obtained from tissue homogenate and normalizing to tissue weight.

IgG ELISA

Supernatants obtained from tissue homogenates (granulomatous lung, normal lung, dLN, and pLN) after necropsy were used to quantify total and *M. tuberculosis*-specific IgG. Tissue culture-grade, 96-well, flat-bottom Costar plates (Corning, Corning, NY) were coated with 2 μg of *M. tuberculosis* culture filtrate protein (CFP) or mouse anti-primate IgG (clone 8F1; NIH Nonhuman Primate Reagent Resource) dissolved in tissue-grade 1× PBS and incubated overnight at 4°C. To block the plates, 1% bovine serum albumin (BSA) in 1× PBS was used, either at room temperature for 2 hours or overnight at 4°C. Samples were plated in duplicate, and serial dilutions were performed at 1:2 with 1% BSA in 1× PBS. Standard curves were generated using purified cynomolgus macaque serum IgG. Horseradish-peroxidase conjugated mouse anti-primate IgG antibody (clone 1B3; NIH Nonhuman Primate Reagent Resource) was used as the detection agent (diluted at 1:5000). 3,3′,5,5′-Tetramethylbenzidine hydrochloride (Sigma-Aldrich, St. Louis, MO) was used as the chromogenic substrate, according to the manufacturer's instructions. All incubations were performed for 1 hour at 37°C unless otherwise stated. All washes were performed with 1× PBS.

Plasma Cell ELISPOT

Ninety-six-well ELISPOT plates (Upstate; Millipore, Billerica, MA) were coated with *M. tuberculosis* CFP, ESAT6 protein (BEI Resources, Manassas, VA), and mouse anti-primate IgG (clone 8F1; NIH Nonhuman Primate Reagent Resource) and then blocked as described above. Cells from tissues obtained during necropsy (bone marrow, granulomatous lung, normal lung, dLN, and pLN) were resuspended to 1×10^6/mL in RPMI 1640 medium (Lonza) supplemented with 1% L-glutamine and 1% HEPES (Sigma-Aldrich) and 1.5×10^5 cells (150 μL) were added into each well and incubated for 16 to 20 hours at 37°C. Horseradish peroxidase-conjugated mouse anti-primate IgG antibody (clone 1B3; NIH Nonhuman Primate Reagent Resource, Boston, MA) was used as the detection agent (diluted at 1:2500) and incubated for 1 hour at 37°C. Each well was developed using 100 μL of 3-amino-9-ethylcarbazole (AEC) prepared according to the manufacturer's instructions (Vector Laboratories). All washes were performed with 1× PBS.

Data Analysis

Flow cytometry data were analyzed with the FlowJo software package version 7.6.4 (Tree Star, Ashland, OR). Imaging data were analyzed using Prism 5 (GraphPad Software, La Jolla, CA). Fluorescent whole granuloma images are composites of 20 to 40 images taken at ×20 magnification and assembled with Adobe Photoshop 7 (Adobe, San Jose, CA). Statistical comparisons were performed using the Mann-Whitney test. Paired samples were analyzed using the Wilcoxon matched-pairs signed rank test. $P < 0.05$ was considered statistically significant.

Results

Lung Granulomas of NHPs Contain Aggregates of B Cells Reminiscent of Germinal Centers

Serial sections of NHP lung granulomas were characterized histologically then stained for CD3 to identify T cells, CD20 to identify B cells, and DRAQ5 to identify cell nuclei. Scattered cells and aggregates of $CD20^+$ cells were observed within the lymphocyte cuff of lung granulomas. $CD3^+$ T cells assumed a more ubiquitous distribution within the granuloma, compared with the clustered appearance of $CD20^+$ B cells, and were observed to be closely associated within the B-cell clusters. $CD3^+$ T cells were also present closer to the center of the granuloma, which was devoid of $CD20^+$ cells (Figure 1A). We hypothesized that the B-cell clusters within the granulomas may be similar to ectopic germinal centers. To determine whether the $CD20^+$ clusters have tertiary germinal center characteristics,[23] we stained for PNA expression (germinal center B cells),[28,29] anti-human Ki-67 (proliferation), and PNAd (high endothelial venules) (Figure 1B). Within a mature germinal center, Ki-67^+ cells tend to cluster at the center of the B-cell follicle, thus delineating actively proliferating cells (Figure 1C). Ki-67^+ nuclei were detected within the lymphocytic cuff, indicating that active cellular proliferation was occurring. Cells with Ki-67^+ nuclei were observed within the $CD20^+$ B-cell clusters in the granu-

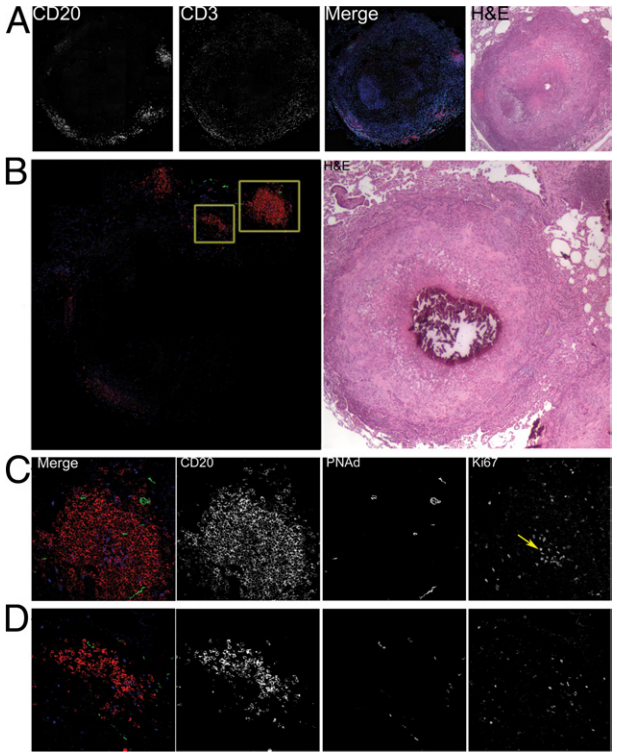

Figure 1. CD20$^+$ B-cell clusters are present within macaque granulomas and have germinal center characteristics. **A:** A solid granuloma (merged image) with some caseum and a small mineralized focus was stained for CD20 (red), CD3 (green), and nuclei with DRAQ5 (blue) to show the distribution of immune cells with respect to granuloma morphology (H&E stain). CD20$^+$ B cells and CD3$^+$ T cells (depicted as CD20 and CD3 grayscale images, respectively) are found primarily within the lymphocytic cuff. B cells generally form clusters, but are also present as discrete cells, whereas T cells are usually dispersed. **B:** A caseous granuloma section with a mineralized core (H&E stain) (**right panel**) was stained for CD20 (red), PNAd (green), and Ki-67 (blue) to identify B cells, high endothelial venules, and proliferating cells, respectively. Two CD20$^+$ clusters were imaged in detail for germinal center markers (**boxed** areas, **left panel**). **C:** A mature bronchus-associated lymphoid tissue cluster exhibits prominent Ki-67 staining within CD20$^+$ cells in close association with PNAd+ high endothelial venules (**arrow**), reminiscent of B-cell follicles within lymph nodes. **D:** B-cell clusters within the lymphocytic cuff of the granuloma contain some Ki-67$^+$ nuclei, with some sporadic PNAd staining. Merged images in **C** and **D** depict CD20 (red), PNAd (green), and Ki-67 (blue). Images shown are composites of 20 to 40 images. Original magnification: ×20 (**B**) or ×40 (**C** and **D**).

loma, but occurred only as isolated cells rather than a distinct cluster (Figure 1D), compared with mature B-cell germinal centers.

PNAd is important for lymphocyte chemotaxis, and positive expression is associated with the presence of high endothelial venules, indicative of germinal centers (Figure 1C). PNAd$^+$ cells were detected in close proximity to CD20$^+$ cells within the lymphocytic cuff of the granuloma (Figure 1D).

PNA is widely used in identifying germinal centers in mouse models, but in the present study of NHP granulomas no PNA staining was noted within the CD20$^+$ clusters; however, strong PNA staining was noted within the macrophage layers of the granuloma. Very weak PNA staining was present within the B-cell follicles of NHP lymph nodes (data not shown). PNA also stains human monocytes, macrophages, and plasma cells (as reported previously[18] and unpublished data). These findings suggest that PNA expression is very different in primates, compared with mice, and we therefore excluded PNA as a germinal center marker. Thus, these data support that concept that the CD20$^+$ clusters in granulomas display some prominent characteristics of ectopic germinal centers. Further characterization of the B cells within the granuloma was performed to assess cellular activation.

CD20$^+$ Cell Clusters within Lung Granulomas Contain Activated B Cells

Flow cytometry was performed on single-cell suspensions of lung and lymph node tissues to assess B-cell numbers within infected tissue. Lymphocytes were identified based on size and granularity, and B cells were further isolated based on CD20$^+$ expression (Figure 2A). CD20$^+$ cells were found to be present at greater numbers within *M. tuberculosis*-infected lung, compared with randomized normal lung samples, on a per-gram basis ($P < 0.005$). No difference in numbers of CD20$^+$ cells was observed between dLN and pLN (Figure 2B).

Increased HLA-DR expression on B cells was used to identify activated B cells within infected tissue, on the premise that activated B cells have enhanced antigen presentation capacity. The frequency of CD20$^+$ cells from dLN or pLN expressing HLA-DR was similar (Figure 2C). However, HLA-DR expression was higher on CD20$^+$ cells from dLN, compared with pLN, within individual animals (animals 19808 and 20908; Figure 2D). Although HLA-DR was demonstrated on cells from involved lung tissue, it was not possible to obtain similar data from uninvolved lung, because insufficient B cells were present within those tissues to allow meaningful analysis. No appreciable difference in CD86 expression could be seen within the CD20$^+$ cells from involved lung samples, compared with uninvolved lung tissue (data not shown).

The chemokine receptor CXCR5 was used to identify activated lymphocytes that respond to trafficking signals into lymphoid tissue. CXCR5 expression was observed on CD20$^+$ B-cell clusters within the granuloma; however, very little colocalization of CD3 and CXCR5 was observed within the lymphocytic cuff of the granuloma (Figure 2E).

Plasma Cells and Antibody Responses to M. tuberculosis*-Specific Antigen within Involved Tissues*

Given that B-cell clusters within the granuloma share many germinal center characteristics, the presence of plasma cells would further support the hypothesis that, within the granuloma, B cells are differentiating *in situ*. Plasma cells were identified within the granuloma based on morphology (clock-faced nuclei; higher cytoplasm to nuclear ratio) from H&E-stained granuloma sections (Figure 3A). Staining for CD138 (a plasma cell marker in humans) was performed on paraformaldehyde-fixed frozen granuloma sections, but it failed to detect any CD138$^+$ plasma cells (data not shown). NHP lymph node samples do contain cells stained positive with CD138 within the B-cell follicles (data not shown).

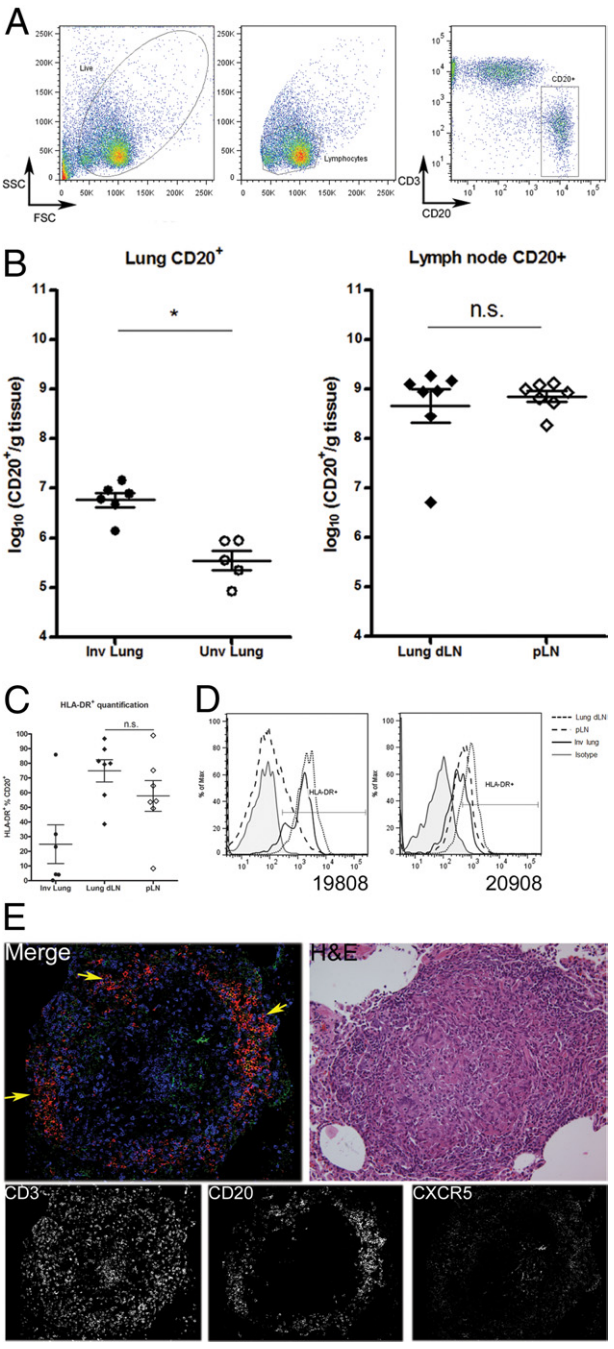

Figure 2. Activated B cells are present in mycobacteria-containing tissue. **A:** Lymphocytes were gated based on size [forward scatter (FSC)] and granularity [side scatter (SSC)]. B cells were further identified based on $CD20^+$ expression. The fluorescence-activated cell sorting FACS plot depicts the cellular profile of a lymph node sample. **B:** Involved lung samples (Inv lung) have at least a 10-fold increase in $CD20^+$ B cells, compared with uninvolved lung samples (Unv lung). B-cell numbers were similar within pLN and dLN. Each data point represents one tissue sample from one macaque. **C:** HLA-DR expression by $CD20^+$ cells from dLN, although slightly elevated, was not significantly different, compared with cells from pLN. **D:** In contrast, analysis of tissues from two representative macaques (19808 and 20908) indicated elevated HLA-DR expression within $CD20^+$ cells of dLN, compared with pLN of the same macaque. $CD20^+$ from involved lung samples also stained positive for HLA-DR (uninvolved lung lacked sufficient B-cell numbers for analysis). **E:** Staining for CD3 (blue), CD20 (red), and CXCR5 (green) was done to determine whether B-cell clusters within the granuloma behave as ectopic germinal centers. CXCR5 was used to identify lymphocytes that are actively homing toward lymphoid tissue to identify germinal center reactions. Most of the B-cell clusters stained positive for CXCR5 (**arrows**), indicating activated $CD20^+$ cells that are capable of homing toward lymphoid tissue. Data are expressed as means ± SEM (**B** and **C**). $^*P < 0.05$. $n = 7$ (**B** and **C**). n.s., nonsignificant.

As another measure of plasma cells, a short-term IgG ELISPOT was used to assess CFP-specific and ESAT6-specific plasma cells within lymph node, lung, and sternum bone marrow samples from seven infected NHPs. Antigen-specific plasma cells for mycobacterial antigens (CFPs and ESAT6) within involved lung samples and for CFP within dLN were present in greater numbers, on average, compared with uninvolved lung samples and pLN, respectively, although the difference did not achieve statistical significance. However, numbers of ESAT6-specific plasma cells were significantly greater in dLN, compared with pLN ($P < 0.05$) (Figure 3B). Numbers of plasma cells specific for CFP and ESAT6 were similar within sternum bone marrow samples (Figure 3C).

To quantitate antibody levels within tissue samples, lung and lymph node supernatants from 14 NHPs were assayed by ELISA for CFP-specific IgG antibodies. Pairwise analysis of involved and uninvolved lung samples from the same NHP also showed an increase in CFP-specific IgG amounts within involved lung supernatants ($P < 0.05$). The same increase was observed within dLN supernatants, compared with pLN samples ($P < 0.01$) (Figure 3D). Total IgG levels were similar within both lung and lymph node groups (data not shown).

Discussion

The importance of B cells in control of human *M. tuberculosis* infection remains unclear, despite numerous studies on antibody responses in humans.[16,30,31] In the present study, we assessed the presence of B cells and antibodies in the granulomas of *M. tuberculosis*-infected macaques, using a model that accurately recapitulates both the pathology (including granuloma types) and infection outcomes seen in humans infected with *M. tuberculosis*. B cells have been demonstrated to contribute to control of *M. tuberculosis* in mouse models,[17] and are reminiscent of germinal centers of lymphoid tissues based on cell organization and chemokine response.[22] However, the structure of murine granulomas is not similar to granulomas seen in humans. Here, we demonstrate that B cells are present as a significant population within NHP lung granulomas and are organized into discrete clusters with germinal center characteristics and numerous plasma cells and activated B cells.

Several studies have suggested that B cells within the granuloma are highly reminiscent of germinal centers, based on surface marker expression.[23,32] Ectopic germinal center formation or lymphoid neogenesis has been closely associated with chronic inflammation in autoimmune and infectious disease settings,[29] and was considered a more efficient way of presenting antigen to drive cellular activation at lesion sites. In the case of the NHP granuloma, the B-cell clusters may be positioned within the lymphocytic cuff evenly, like the black spots on a white soccer ball. This may help drive antigen presentation for T-cell activation, given the similarities of granuloma B-cell clusters to lymph node germinal centers and the increased HLA-DR expression present on involved lung B cells. Further functional analysis may determine

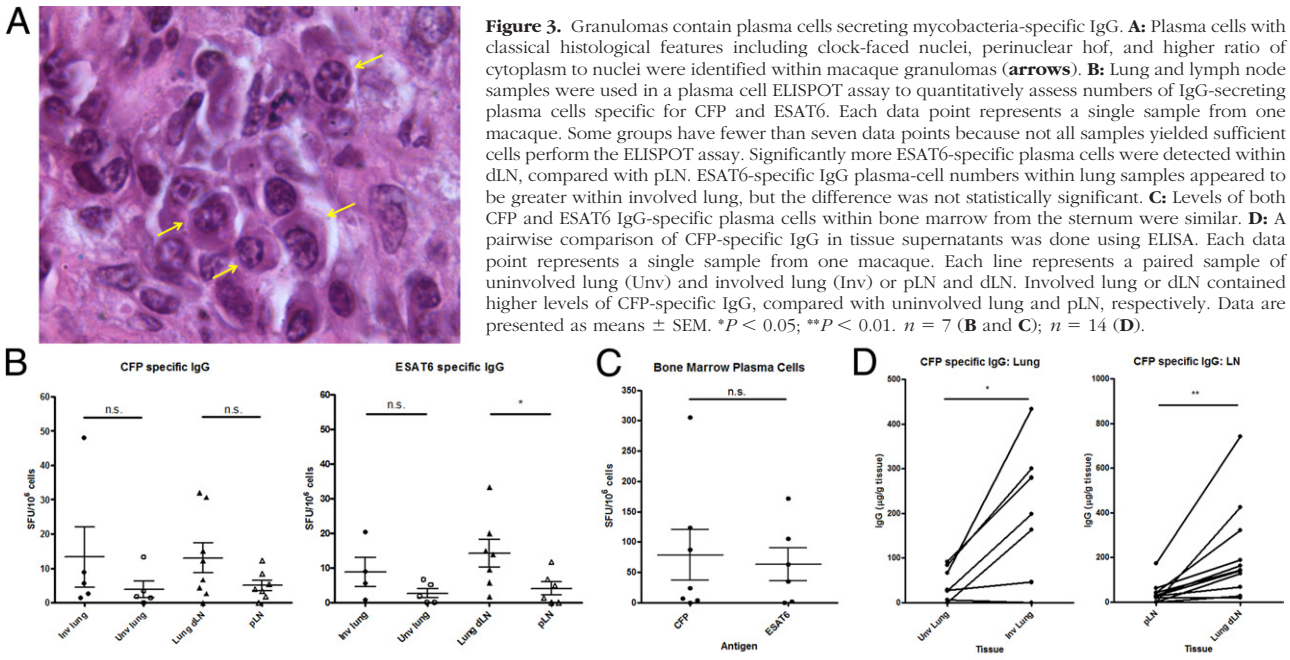

Figure 3. Granulomas contain plasma cells secreting mycobacteria-specific IgG. **A:** Plasma cells with classical histological features including clock-faced nuclei, perinuclear hof, and higher ratio of cytoplasm to nuclei were identified within macaque granulomas (**arrows**). **B:** Lung and lymph node samples were used in a plasma cell ELISPOT assay to quantitatively assess numbers of IgG-secreting plasma cells specific for CFP and ESAT6. Each data point represents a single sample from one macaque. Some groups have fewer than seven data points because not all samples yielded sufficient cells perform the ELISPOT assay. Significantly more ESAT6-specific plasma cells were detected within dLN, compared with pLN. ESAT6-specific IgG plasma-cell numbers within lung samples appeared to be greater within involved lung, but the difference was not statistically significant. **C:** Levels of both CFP and ESAT6 IgG-specific plasma cells within bone marrow from the sternum were similar. **D:** A pairwise comparison of CFP-specific IgG in tissue supernatants was done using ELISA. Each data point represents a single sample from one macaque. Each line represents a paired sample of uninvolved lung (Unv) and involved lung (Inv) or pLN and dLN. Involved lung or dLN contained higher levels of CFP-specific IgG, compared with uninvolved lung and pLN, respectively. Data are presented as means ± SEM. $^{*}P < 0.05$; $^{**}P < 0.01$. $n = 7$ (**B** and **C**); $n = 14$ (**D**).

the ability of B cells from granulomas to present mycobacterial antigens and activate T-cell responses, as well as the relative efficiency of granuloma B cells for these processes, compared with peripheral B cells.

The increased amount of antigen-specific IgG at the site of infection lends support to the notion that antibodies may modulate the host-pathogen interactions in the granuloma. Antigen-specific IgG-secreting plasma cells present within lung granulomas suggest that substantial antibody production is occurring; however, a much greater increase of both antigen-specific IgG and plasma cells was noted within dLN, which indicates that *M. tuberculosis*-specific plasma cells are being generated and possibly retained within dLN. These lymph nodes are often infected, and usually contain *M. tuberculosis*-specific T cells.[25,26] It is highly likely that the plasma cells in involved lung tissues are derived from activated B cells that are recruited to the granulomas. Upon fully differentiating into plasma cells, these terminally differentiated B cells likely gain CD138 expression and migrate back to the bone marrow. This would explain the absence of $CD138^{+}$ cells within the granuloma. Although B-cell clusters within the granuloma share many characteristics with lymph node germinal centers, the granuloma B-cell clusters contain far fewer B cells, making detection of mature CD138-expressing cells less likely.

The role of antibody remains unclear in TB. Historically, passive immunization and serum therapy have yielded conflicting results in human patients. Studies in humans have been confined largely to using *M. tuberculosis*-specific antibodies as indicators of disease states by measuring serum IgG specific to *M. tuberculosis* antigens.[30,31,33] However, there may be a role for antibodies at the site of infection. One hypothesis is that antibody-coated (extracellular) *M. tuberculosis* bacilli engage Fcγ receptors (FcγR) rather than just DC-SIGN and complement receptors, resulting in increased macrophage activation.[8,34] These changes are likely mediated by cross-linking of Fcγ receptors expressed on macrophages and neutrophils by immune complexes of IgG and *M. tuberculosis* bacilli. Data from *M. tuberculosis*-infected Fcγ receptor knockout mice also suggest that antibody-mediated events are involved in the anti-TB response.[19] Given that macrophage activation is essential for control of *M. tuberculosis*, antibodies may play a role in regulating macrophage function within the granuloma. Nonetheless, antibody-mediated phagocytosis may not necessarily be protective, as demonstrated in dengue fever or Coxsackie B infection.[10] In rabbits infected with *M. tuberculosis*, increased B-cell activation was observed to be associated with failure to contain the disease.[35] Antibody-dependent enhancement of infection may also play a role in exacerbating the course of infection for *M. tuberculosis*.

Our present findings demonstrate that activated B cells, plasma cells, and antibodies are enriched within the granuloma, and have some characteristics of germinal centers. Further studies are underway to focus on defining the protective, pathological, or immune modulatory roles for these cells in TB.

Acknowledgments

We thank Drs. Edwin Klein and Chris Janssen for performing necropsies and histological analyses, Mark Rodgers, Catherine Cochran, Melanie O'Malley, Jamie Tomko, Dan Filmore, Carolyn Bigbee, Matthew Bigbee, and Paul Johnston for technical assistance, Dr. John Chan (Albert Einstein College of Medicine) for intellectual discussions, Dr. Keith Reimann (Beth Israel Deaconess Medical Center, Harvard University) for anti-primate specific reagents,

and Dr. Geetha Chalasani (University of Pittsburgh) for peanut agglutinin lectin.

References

1. Wright A, Zignol M; WHO staff: Anti-Tuberculosis Drug Resistance in the World. Fourth global report. The WHO/IUATLD Global Project on Anti-tuberculosis Drug Resistance Surveillance 2002–2007. Geneva: WHO Press, 2008
2. Brewer TF, Heymann SJ: To control and beyond: moving towards eliminating the global tuberculosis threat. J Epidemiol Community Health 2004, 58:822–825
3. Maartens G, Wilkinson RJ: Tuberculosis. Lancet 2007, 370:2030–2043
4. Saunders BM, Britton WJ: Life and death in the granuloma: immunopathology of tuberculosis. Immunol Cell Biol 2007, 85:103–111
5. Scanga CA, Mohan VP, Yu K, Joseph H, Tanaka K, Chan J, Flynn JL: Depletion of CD4(+) T cells causes reactivation of murine persistent tuberculosis despite continued expression of interferon gamma and nitric oxide synthase 2. J Exp Med 2000, 192:347–358
6. Zhang SY, Boisson-Dupuis S, Chapgier A, Yang K, Bustamante J, Puel A, Picard C, Abel L, Jouanguy E, Casanova JL: Inborn errors of interferon (IFN)-mediated immunity in humans: insights into the respective roles of IFN-alpha/beta, IFN-gamma, and IFN-lambda in host defense. Immunol Rev 2008, 226:29–40
7. Willcocks LC, Smith KG, Clatworthy MR: Low-affinity Fcgamma receptors, autoimmunity and infection. Expert Rev Mol Med 2009, 11: e24
8. de Vallière S, Abate G, Blazevic A, Heuertz RM, Hoft DF: Enhancement of innate and cell-mediated immunity by antimycobacterial antibodies. Infect Immun 2005, 73:6711–6720
9. Gallo P, Gonçalves R, Mosser DM: The influence of IgG density and macrophage Fc (gamma) receptor cross-linking on phagocytosis and IL-10 production. Immunol Lett 2010, 133:70–77
10. Halstead SB, Mahalingam S, Marovich MA, Ubol S, Mosser DM: Intrinsic antibody-dependent enhancement of microbial infection in macrophages: disease regulation by immune complexes. Lancet Infect Dis 2010, 10:712–722
11. Kleindienst P, Brocker T: Concerted antigen presentation by dendritic cells and B cells is necessary for optimal CD4 T-cell immunity in vivo. Immunology 2005, 115:556–564
12. Dörner T: Crossroads of B cell activation in autoimmunity: rationale of targeting B cells. J Rheumatol Suppl 2006, 77:3–11
13. Monson NL, Cravens P, Hussain R, Harp CT, Cummings M, de Pilar Martin M, Ben LH, Do J, Lyons JA, Lovette-Racke A, Cross AH, Racke MK, Stüve O, Shlomchik M, Eagar TN: Rituximab therapy reduces organ-specific T cell responses and ameliorates experimental autoimmune encephalomyelitis. PLoS One 2011, 6:e17103
14. Meinl E, Derfuss T, Krumbholz M, Pröbstel AK, Hohlfeld R: Humoral autoimmunity in multiple sclerosis. J Neurol Sci 2011, 306:180–182
15. Mariño E, Silveira PA, Stolp J, Grey ST: B cell-directed therapies in type 1 diabetes. Trends Immunol 2011, 32:287–294
16. Abebe F, Bjune G: The protective role of antibody responses during Mycobacterium tuberculosis infection. Clin Exp Immunol 2009, 157: 235–243
17. Maglione PJ, Xu J, Chan J: B cells moderate inflammatory progression and enhance bacterial containment upon pulmonary challenge with Mycobacterium tuberculosis. J Immunol 2007, 178:7222–7234
18. Erber WN, Asbahr H, Meyer B, Herrmann RP, Davies JM: Peanut agglutinin (lectin from Arachis hypogaea) binding to hemopoietic cells: an immunophenotypic study using a biotin streptavidin technique. Pathology 1992, 24:173–176
19. Maglione PJ, Xu J, Casadevall A, Chan J: Fc gamma receptors regulate immune activation and susceptibility during Mycobacterium tuberculosis infection. J Immunol 2008, 180:3329–3338
20. Tjärnlund A, Rodríguez A, Cardona PJ, Guirado E, Ivanyi J, Singh M, Troye-Blomberg M, Fernández C: Polymeric IgR knockout mice are more susceptible to mycobacterial infections in the respiratory tract than wild-type mice. Int Immunol 2006, 18:807–816
21. Roy E, Stavropoulos E, Brennan J, Coade S, Grigorieva E, Walker B, Dagg B, Tascon RE, Lowrie DB, Colston MJ, Jolles S: Therapeutic efficacy of high-dose intravenous immunoglobulin in Mycobacterium tuberculosis infection in mice. Infect Immun 2005, 73:6101–6109
22. Kahnert A, Höpken UE, Stein M, Bandermann S, Lipp M, Kaufmann SH: Mycobacterium tuberculosis triggers formation of lymphoid structure in murine lungs. J Infect Dis 2007, 195:46–54
23. Ulrichs T, Kosmiadi GA, Trusov V, Jörg S, Pradl L, Titukhina M, Mishenko V, Gushina N, Kaufmann SH: Human tuberculous granulomas induce peripheral lymphoid follicle-like structures to orchestrate local host defence in the lung. J Pathol 2004, 204:217–228
24. Tsai MC, Chakravarty S, Zhu G, Xu J, Tanaka K, Koch C, Tufariello J, Flynn J, Chan J: Characterization of the tuberculous granuloma in murine and human lungs: cellular composition and relative tissue oxygen tension. Cell Microbiol 2006, 8:218–232
25. Capuano SV 3rd, Croix DA, Pawar S, Zinovik A, Myers A, Lin PL, Bissel S, Fuhrman C, Klein E, Flynn JL: Experimental Mycobacterium tuberculosis infection of cynomolgus macaques closely resembles the various manifestations of human M. tuberculosis infection. Infect Immun 2003, 71:5831–5844
26. Flynn JL, Capuano SV, Croix D, Pawar S, Myers A, Zinovik A, Klein E: Non-human primates: a model for tuberculosis research. Tuberculosis (Edinb) 2003, 83:116–118
27. Lin PL, Pawar S, Myers A, Pegu A, Fuhrman C, Reinhart TA, Capuano SV, Klein E, Flynn JL: Early events in Mycobacterium tuberculosis infection in cynomolgus macaques. Infect Immun 2006, 74:3790–3803
28. Maglione PJ, Chan J: How B cells shape the immune response against Mycobacterium tuberculosis. Eur J Immunol 2009, 39:676–686
29. Aloisi F, Pujol-Borrell R: Lymphoid neogenesis in chronic inflammatory diseases. Nat Rev Immunol 2006, 6:205–217
30. Khan IH, Ravindran R, Krishnan VV, Awan IN, Rizvi SK, Saqib MA, Shahzad MI, Tahseen S, Ireton G, Goulding CW, Felgner P, DeRiemer K, Khanum A, Luciw PA: Plasma antibody profiles as diagnostic biomarkers for tuberculosis. Clin Vaccine Immunol 2011, 18:2148–2153
31. Reis MC, Silva BD, Sousa EM, Junqueira-Kipnis AP: Role of antibodies reactive to HspX in discriminating pulmonary tuberculosis contacts with high risk of developing active disease. Braz J Infect Dis 2011, 15:617–618
32. Zhang M, Wang Z, Graner MW, Yang L, Liao M, Yang Q, Gou J, Zhu Y, Wu C, Liu H, Zhou B, Chen X: B cell infiltration is associated with the increased IL-17 and IL-22 expression in the lungs of patients with tuberculosis. Cell Immunol 2011, 270:217–223
33. Khan IH, Ravindran R, Yee J, Ziman M, Lewinsohn DM, Gennaro ML, Flynn JL, Goulding CW, DeRiemer K, Lerche NW, Luciw PA: Profiling antibodies to Mycobacterium tuberculosis by multiplex microbead suspension arrays for serodiagnosis of tuberculosis. Clin Vaccine Immunol 2008, 15:433–438
34. Dheda K, Booth H, Huggett JF, Johnson MA, Zumla A, Rook GA: Lung remodeling in pulmonary tuberculosis. J Infect Dis 2005, 192: 1201–1209
35. Subbian S, Tsenova L, Yang G, O'Brien P, Parsons S, Peixoto B, Taylor L, Fallows D, Kaplan G: Chronic pulmonary cavitary tuberculosis in rabbits: a failed host immune response. Open Biol 2011, 1:110016